Structural Engineering and Mechanics, *Vol. 73, No. 3 (2020) 339-351*
DOI: https://doi.org/10.12989/sem.2020.73.3.339

A comprehensive approach to flow-based seismic risk analysis of water transmission network

Sungsik Yoon[1a], Young-Joo Lee[2b] and Hyung-Jo Jung[∗1]

[1]Department of Civil and Environmental Engineering, Korea Advanced Institute of Science and Technology, 291 Daehak-ro, Yuseong-gu, Daejeon 34141, Republic of Korea
[2]School of Urban and Environmental Engineering, Ulsan National Institute of Science and Technology, 50 UNIST-gil, Eonyang-eup, Ulju-gun, Ulsan 44919, Republic of Korea

(Received May 31, 2019, Revised October 10, 2019, Accepted October 11, 2019)

Abstract. Earthquakes are natural disasters that cause serious social disruptions and economic losses. In particular, they have a significant impact on critical lifeline infrastructure such as urban water transmission networks. Therefore, it is important to predict network performance and provide an alternative that minimizes the damage by considering the factors affecting lifeline structures. This paper proposes a probabilistic reliability approach for post-hazard flow analysis of a water transmission network according to earthquake magnitude, pipeline deterioration, and interdependency between pumping plants and 154 kV substations. The model is composed of the following three phases: (1) generation of input ground motion considering spatial correlation, (2) updating the revised nodal demands, and (3) calculation of available nodal demands. Accordingly, a computer code was developed to perform the hydraulic analysis and numerical modelling of water facilities. For numerical simulation, an actual water transmission network was considered and the epicenter was determined from historical earthquake data. To evaluate the network performance, flow-based performance indicators such as system serviceability, nodal serviceability, and mean normal status rate were introduced. The results from the proposed approach quantitatively show that the water network is significantly affected by not only the magnitude of the earthquake but the interdependency and pipeline deterioration.

Keywords: water transmission network; flow-based network simulation; seismic risk analysis; water network interdependency; buried pipeline deterioration

1. Introduction

In recent times, frequent earthquakes have caused human casualties and property damage, resulting in increased social disruption. The critical lifeline infrastructure throughout the city can be directly or indirectly damaged, and it causes significant difficulties in daily life. The Northridge earthquake (1994) in California, USA and the Kobe earthquake (1995) in Japan led to immense damage to waterworks facilities. The Northridge earthquake (M 6.7) resulted in approximately 74 breaks to the main pipeline of diameter over 600 mm and 1013 breaks in the main pipeline below the diameter of 600 mm. In Kobe earthquake (M 6.9), there were 23 breaks to the main water line, limiting the water supply to approximately 15 million people. In addition, the Kaikoura earthquake (M 7.8) in New Zealand (2016) had a significant economic impact on other lifelines (indirect losses) as well as the water lifeline itself (direct losses).

Water supply facilities are mainly buried underground, making it difficult to detect damage points, which can lead to long-term economic isolation (Kim *et al.* 2019). Recent earthquakes have highlighted the need for damage prediction and disaster preparedness. The possibility of strong ground motion is not high, but if it occurs, it can cause immense damage to waterworks facilities. Therefore, proactive seismic risk assessment of water networks should be undertaken. Accordingly, several researchers conducted seismic risk analysis on various critical lifelines based on connectivity analysis. For example, Esposito *et al.* (2015) conducted simulation-based seismic risk assessment of the gas distribution network of L'Aquila in central Italy, including gas network facilities such as metering/pressure reduction stations. Song and Ok (2010) evaluated the system reliability of the gas network of Shelby County of Tennessee, USA using a network decomposition approach with matrix-based system reliability. Moreover, Rokneddin *et al.* (2013) evaluated the system reliability and bridge ranking of bridge networks through O-D (Origin-Destination) connectivity based on Markov Chain Monte Carlo (MCMC) simulations. In the case of water supply networks, Fragiadakis and Christodoulou (2014) proposed the failure probability of a pipeline according to the elapsed time through the survival function and evaluated the network performance of the water supply network in Limassol, Cyprus. Dueñas-Osorio *et al.* (2007) conducted a

∗Corresponding author, Professor
E-mail: hjung@kaist.edu
[a] Ph.D. Student
E-mail: yss3366@kaist.ac.kr
[b] Associate Professor
E-mail: ylee@unist.ac.kr

http://www.techno-press.com/journals/sem&subpage=7
ISSN: 1225-4568 (Print), 1598-6217 (Online)

reliability analysis of the interdependence of water networks considering the impact of the power network on the water network, and proposed mitigation actions to reduce the network damage. Lim and Song (2012) used a selective recursive decomposition algorithm to evaluate the post-disaster responses of Shelby County of Tennessee, USA. Furthermore, Yoon *et al*. (2018) presented a comprehensive framework for evaluating connectivity-based network performance and conducted a seismic risk assessment of A-city located in South Korea.

In addition, the network performance has been evaluated based on the flow equation for various lifeline facilities. Lee *et al*. (2011) evaluated the post-hazard flow capacity of a bridge network located in Sioux Falls, USA, considering bridge deterioration. Sánchez-Silva *et al*. (2005) proposed a model for the efficient assignment of resources based on the reliability of the transportation network. In case of the water supply networks, numerous studies have been conducted using numerical analysis programs developed by the US Environmental Protection Agency (EPA) (EPANET) and Shi and O'Rourke (2006) (GIRAFFE). Y. Wang and O'Rourke (2006) utilized GIRAFFE to evaluate the seismic performance of five water districts in the Los Angeles (LA) region, and Bonneau and O'Rourke (2009) used the improved hydraulic network model to evaluate the performance of the LA water supply system during earthquakes and extreme events. Furthermore, Yoo *et al*. (2015) evaluated the seismic response of I city and J city in South Korea using EPANET. Moreover, Romero *et al*. (2010) proposed a strategy to respond to emergencies efficiently by evaluating the system reliability of seismic hazards in the LA area, and Kang *et al*. (2017) proposed a framework employing EPANET for a reliability-based flow analysis of a water pipe network after an earthquake.

Most of the previous studies proposed efficient numerical methods based on connectivity algorithms and performance evaluation considering integrated factors. However, the connectivity-based network analysis has a limitation in seismic risk analysis, because it is impossible to represent realistic hydraulic modelling of water networks. Therefore, for accurate seismic risk analysis of a water transmission network, the performance of the network should be evaluated based on flow analysis that reflects each numerical method including spatially correlated ground motion prediction equation (GMPE), consideration of buried pipeline deterioration, the interdependency of power facilities and water facilities, and the numerical modelling of water network facilities and leakage/breakage buried pipe. Thus, we propose a comprehensive approach to evaluate the flow-based seismic performance of an urban water transmission network. The proposed probabilistic reliability model consists of an earthquake generation model and hydraulic analysis model, and the performance of water networks was evaluated using performance indicators according to the magnitude of the earthquake, elapsed time of pipeline, and interdependency. For this purpose, the actual A-city water transmission network was set as a benchmark network to apply the probabilistic reliability model, as A-city is vulnerable to ground shaking owing to recent earthquakes.

2. Research background

2.1 Network analysis

2.1.1 Connectivity analysis

A lifeline can be represented using a network system, and connectivity-based and flow-based methods are often used for network analysis. Connectivity analysis is based on topology without regarding the condition of the nodes and links. However, it has a limitation in seismic risk analysis, because it only identifies the connectivity between the source and sink nodes by classifying the damage state of the link into two discrete states: a normal state and a failure state. In general, connectivity-based network analysis is represented by graph theory (Ahuja *et al.* 1993) and is known to be a powerful mathematical tool for easily controlling complex network data. The graph theory is constructed with nodes and links—denoted by V and E, respectively—and it can be divided into direct graphs and indirect graphs depending on the flow path between two nodes (v1, v2). In addition, the network connectivity is represented by an adjacency matrix of size $N \times N$, and the elements of the adjacency matrix are determined as 0 or 1, depending on whether the two nodes are connected or not. Based on the constructed network information, graph theory allows the user to identify the shortest paths or connections between two nodes efficiently using various path-finding algorithms on a complex network. Previous studies have applied the connectivity approach to a power network (Dueñas-Osorio *et al.* 2007), bridge network (Rokneddin *et al.* 2013), water supply network (Fragiadakis and Christodoulou, 2014; Yoon *et al.* 2018), and gas network (Esposito *et al.* 2015; Song and Ok, 2010). However, as connectivity-based approaches tend to overestimate the performance of the network (Farahmandfar and Piratla, 2017), a more sophisticated, flow-based approach must be implemented for more accurate assessment.

2.1.2 Flow-based analysis

The flow-based approach is a network analysis method that reflects the serviceability and capacity of nodes and links according to the physical states. In contrast to the connectivity-based method, the function of each node and link can be evaluated using a flow equation, allowing accurate performance evaluation between the source and sink nodes. Therefore, when external disturbances such as earthquakes occur, topology-based connections and additional flow analysis are required to evaluate the performance of each node and link. The flow-based approach is more accurate than the connectivity-based method, but its computational cost is higher, and hence, proper adoption of this approach is required. Numerous prior studies have applied flow-based approaches to various lifeline systems, including a power network (Nuti *et al.* 2010), bridge networks (Lee *et al.* 2011), water networks (Romero *et al.* 2010; Yoo *et al.* 2015, Kashani *et al*, 2016), and gas networks. In the case of water supply networks, EPANET, which is a network analysis software developed by the US EPA, is used in combination with geographic information system (GIS). Recently, it has been used in conjunction with external programming languages such as

C/C++ and MATLAB computer code. The EPANET program represents water facilities through a link (buried pipe, pumping plant) and a node (water treatment plant, water storage tank), and the physical input information (e.g., elevation, pipe diameter, pipe roughness, pressure, etc.) on each facility is considered to enable the assessment of hydraulic behaviour in the network. Thus, this study evaluated the performance of a water supply network based on the interface of EPANET analysis with MATLAB environment.

2.2 Ground motion prediction equation (GMPE)

Ground motion represents the shaking of ground surface as the energy within the earth is transmitted to the surface. With the release of energy, various types of ground motions can be generated depending on the transmitted paths and geological characteristics. However, as the phenomenon of energy radiation during fault rupture is physically complex, a mathematically simple expression is required, which is called GMPE. The general form of GMPE can be expressed as a function of the epicenter location, site location, transmitted path, and characteristics and types of the ground (Joyner and Boore, 1993) as follows:

$$Y_{ij}(T_n) = \overline{Y_{ij}(M_i, R_{ij}, \xi_{ij}, T_n)} + \eta_i(T_n) + \epsilon_{ij} \tag{1}$$

where $Y_{ij}(T_n)$ represents the ground motion intensity including the peak ground acceleration (PGA), peak ground velocity (PGV), and peak ground deformation (PGD) at the j site owing to the vibration period T_n at the epicenter i, M is the magnitude of the earthquake, R_{ij} is the distance between i and j, ξ_{ij} is the geomorphic factor affecting the ground motion, and $\overline{Y_{ij}(M_i, R_{ij}, \xi_{ij}, T_n)}$ represents the mean ground motions. $\eta_i(T_n)$ and $\epsilon_{ij}(T_n)$ represent inter- and intra-events, respectively, which indicate the uncertainty of the ground motion. The inter-event represents the uncertainty of the ground motion owing to the inherent characteristics of the earthquake, whereas the intra-event indicates the uncertainty of the ground motion owing to the energy paths and geological characteristics. Therefore, the inter-event is site-independent, whereas the intra-event can generate spatially correlated ground motions depending on the location of the site.

For water supply facilities such as a water treatment plant, water storage tank, and water pumping plant, PGA is known to be suitable for predicting the failure probability, whereas PGV is known as the intensity measure for predicting the failure probability of buried pipelines (FEMA 2003). In this study, PGV and PGA were predicted using the GMPE proposed by Wang and Takada (2005) and Kawashima *et al.* (1984), respectively. Each proposed GMPE is as follows:

$$\begin{aligned} log(PGV_j) &= 0.725M_i + 0.00318H - 0.519 \\ &\quad - 1.318\, log(R_{ij} + 0.334e^{0.653M_i}) \end{aligned} \tag{2}$$

$$PGA_j = 403.8 \text{ x } 10^{0.265M_i} \text{ x } (R_{ij} + 30)^{-1.218} \tag{3}$$

where H is the length of the focal depth (km), and PGA (cm/s^2) and PGV (cm/s) represent the ground motion intensity.

Inter- and intra-events, which indicate the uncertainty of the ground motion, have been studied in various regions such as California (Goda and Hong 2008), Taiwan (Sokolov *et al.* 2010), and Japan (Goda and Atkinson 2009). The uncertainty of ground motions can be expressed by the following equation:

$$\rho_{Total} = \eta_i(T_n) + \epsilon_{ij}(T_n) \tag{4}$$

where

$$\eta_j = \frac{\sigma_\eta^2}{\sigma_\eta^2 + \sigma_\varepsilon^2}, \quad \epsilon_{ij} = \frac{\sigma_\varepsilon^2}{\sigma_\eta^2 + \sigma_\varepsilon^2}\rho(\Delta_{ij}) \tag{5}$$

indicate the inter- and intra-event terms, respectively; σ_η^2 and σ_ε^2 are inter- and intra-event residuals, respectively; $\rho(\Delta_{ij})$ represents the spatial correlation equation. In this study, the spatial correlation relation proposed by Goda and Hong (2008) is utilized as follows:

$$\rho(\Delta_{ij}) = e^{(-0.509\sqrt{\Delta})} \tag{6}$$

where Δ_{ij} is the distance between sites i and j.

2.3 Performance indicator

If the failure probability of a water supply facility is determined by the intensity measure, the performance of the entire network system can be evaluated through hydraulic analysis. As many factors can be considered when assessing the network based on the capacity or demand of the components, it is important to choose the appropriate performance indicator that considers the factors that have a significant impact on the system. In this study, the system serviceability index (S_S) (Wang *et al.* 2010) and the nodal serviceability index ($N_{S,i}$) (Cullinane *et al.* 1992), which are known to be reliable factors of water supply systems, are utilized. System serviceability and nodal serviceability can be expressed as the ratio of the required flow rate and the available flow rate of each node, and when the required nodal flow is 0, the pressure is utilized as a performance measure. The computation of the two proposed reliability factors is as follows:

$$S_S = \frac{\sum_{i=1}^{n} Q_{avl,i}}{\sum_{i=1}^{n} Q_{req,i}} \tag{7}$$

where n represents the number of nodes, $Q_{req,i}$ represents the required flow rate of the i-th node, and $Q_{avl,i}$ represents the available flow rate of the i-th node.

$$N_{S,i} = \begin{cases} \dfrac{Q_{avl,i}}{Q_{req,i}} & if\ Q_{req,i} \neq 0 \\ \sqrt{\dfrac{Min(P_{avl,i}, P_{min,i})}{P_{min,i}}} & if Q_{req,i} = 0 \end{cases} \tag{8}$$

where $P_{avl,i}$ represents the available nodal pressure of the i-th node and $P_{min,i}$ represents the minimum required nodal pressure of the i-th node. In addition, the following four reliability factors were considered to evaluate the normal status and mean normal status of networks facilities (link, pump, tank, and water treatment plant) (Yoo *et al*. 2015):

$$NSL_j = \frac{NS_{L,j}}{TN_L} \tag{9}$$

$$MNSL = \frac{\sum_{j=1}^{N_{MCS}} NSL_j}{N_{MCS}} \tag{10}$$

where $NS_{L,j}$ denotes the number of normal statuses of links in the j-th Monte Carlo simulation (MCS) analysis, TN_L denotes the total number of links, and N_{MCS} denotes the total number of MCS analyses.

$$NSP_j = \frac{NS_{P,j}}{TN_P} \tag{11}$$

$$MNSP = \frac{\sum_{j=1}^{N_{MCS}} NSP_j}{N_{MCS}} \tag{12}$$

where $NS_{P,j}$ represents the number of normal statuses of pumps in the j-th MCS analysis and TN_P represents the total number of pumps.

$$NST_j = \frac{NS_{T,j}}{TN_T} \tag{13}$$

$$MNST = \frac{\sum_{j=1}^{N_{MCS}} NST_j}{N_{MCS}} \tag{14}$$

where $NS_{T,j}$ represents the number of normal statuses of tanks in the j-th MCS analysis and TN_T represents the total number of tanks.

$$NSWTP_j = \frac{NS_{WTP,j}}{TN_{WTP}} \tag{15}$$

$$MNSWTP = \frac{\sum_{j=1}^{N_{MCS}} NSWTP_j}{N_{MCS}} \tag{16}$$

where $NS_{WTP,j}$ represents the number of normal statuses of water treatment plants in the j-th MCS analysis and TN_{WTP} represents the total number of water treatment plants. The four proposed reliability indicators facilitate quantitative assessment of the mean damage rate of each waterworks facility.

3. Numerical modelling of water transmission network

3.1 Water network facilities

3.1.1 Water treatment plant

A water treatment plant purifies water arriving from a water intake structure and improves water quality. In the network analysis, the water treatment plant serves as a source node. According to the US Federal Emergency Management Agency (FEMA, 2003), water treatment facilities are classified into large-scale, medium-scale, and small-scale facilities depending on their water purification capacity and are classified into five damage status—no damage, minor, moderate, extensive, complete—depending on their operation status. In this study, the performance condition of the water treatment plant was considered as the extensive damage state, which is more severe than the short-term malfunction condition but less severe than a complete collapse. Fig. 1(a) shows the failure probability depending on the PGA intensity of the medium-scale water treatment plant. The normal status of the water treatment plant is determined by comparing the calculated failure probability with a random number generated between 0 and 1. If the water treatment plant has been destroyed in accordance with the earthquake simulation, the water supply pressure is regarded as zero to reflect the water treatment facility in the hydraulic modelling. The two water treatment plants used in this study were of medium scale, and the subcomponents were considered to be in the unanchored state.

3.1.2 Water storage tank

A water storage tank is a sink node that stores water sent from a water treatment plant. According to FEMA (2003), the failure probability of a water storage tank is determined by the material type (concrete, steel, wood) and building type (on-ground or underground), considering the typical capacity of a reservoir of 0.5–2 mgd. The damage status of the storage tank was determined to be extensive damage, indicating that the system is severely damaged and out of service. Fig. 1(b) shows the failure probability of a storage tank depending on the material types. To determine the failure status of a storage tank in EPANET, if the storage tank is destroyed by the generated earthquake, the nodal demand is treated as 0 and the supply of flow is modelled to be impossible. The 23 storage tanks used in this study were all made of concrete and were considered to have unanchored status.

3.1.3 Water pumping plant

The waterworks facilities are constructed with pipe channels and represent the system in which the flow rate is determined by the pressure of the nodes. Therefore, additional pressure must be supplied to deliver purified water from a lower-elevation node to a higher-elevation node. The water pumping plant pressurizes the water supplied from the water treatment plant and transfers it to the storage tank. The pumping plant is composed of the building, pump, and power plant and is classified into two types, small pumping plant (capacity less than 10 mgd) and medium/large pumping plant (capacity more than 10 mgd), depending on the capacity of water supplied (FEMA, 2003). Extensive damage was considered as the failure condition of the pumping plant, which indicates that the pump is damaged and cannot be repaired in a short period. In the case of a pumping plant, it is necessary to consider the failure probability of the pumping plant itself as well as the interdependency between the substation and the pumping plant. This is because power is supplied from the substation. The interdependency can be considered using conditional

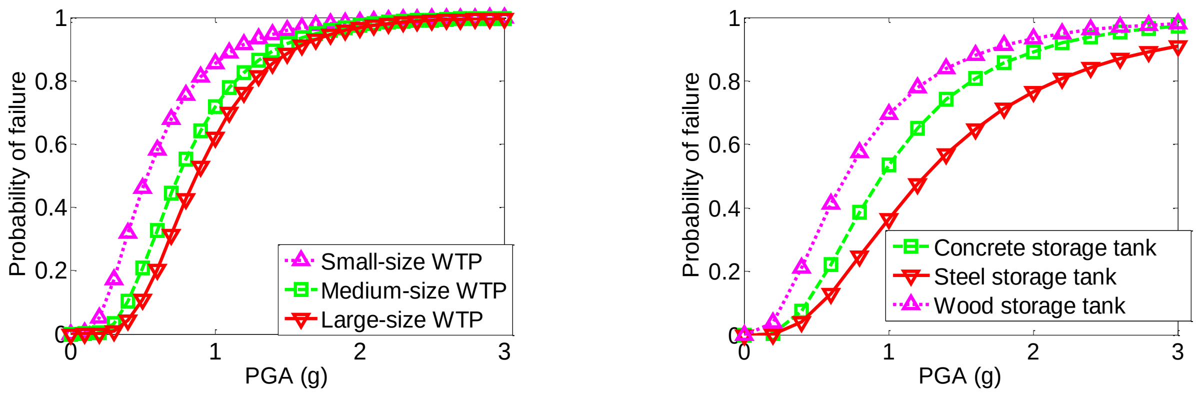

(a) Water treatment plant (b) Water storage tank

Fig. 1 Failure probability of water network facilities

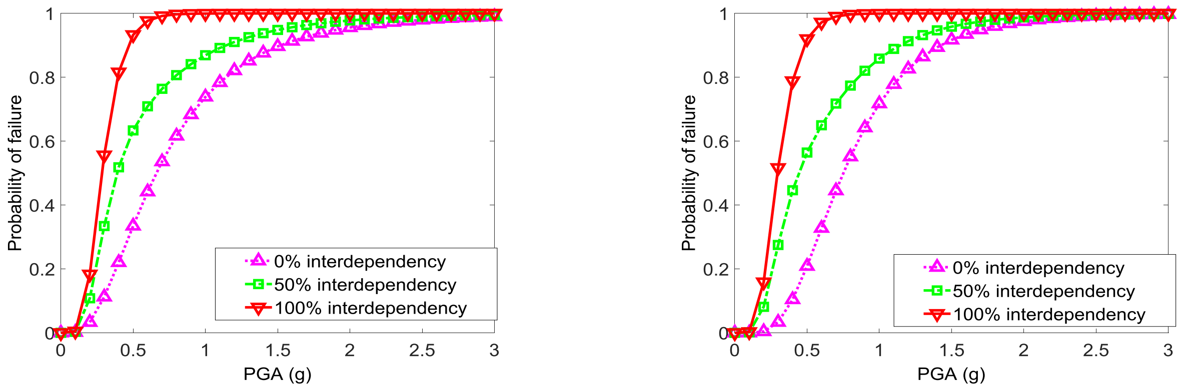

(a) Small pumping plant (b) Medium/Large pumping plant

Fig. 2 Failure probability of water pumping plant according to interdependency

probability, and the effect of interdependency is considered with the conditional probabilities 0, 0.5, and 1. The failure probability that the j-th pumping plant is destroyed when the i-th substation is destroyed can be expressed as

$$P\left(P_j^{inter} \middle| S_i^{earth}\right) = P_{P_j|S_i} \tag{17}$$

where S_i^{earth} denotes the failure probability of the i-th substation owing to the earthquake, and P_j^{inter} denotes the failure probability of the j-th pumping plant located near the i-th substation. Fig. 2 shows the failure probability of a small pumping plant and a medium/large pumping plant with interdependency. When the intensity of the earthquake is small, the failure probability does not change significantly with the interdependency. However, as the intensity of ground motion increases, the failure probability increases rapidly with the interdependency. Therefore, when considering the normal status of the pumping plant, it is necessary to calculate the failure probability considering the influence of the substation. In the EPANET analysis, numerical modelling was performed by designating the state of the pumping plant as closed.

3.2 Buried pipeline

3.2.1 Failure probability of buried pipeline

The buried pipeline transfers purified water from the source node to the sink node and is composed of various materials and diameters depending on the working conditions. FEMA presented the failure probability of a buried pipeline (FEMA, 2003), and the vulnerability of a pipeline is expressed as the repair rate (number of failures per unit pipe length) according to historical earthquake records. In general, pipe breakage caused by ground shaking (seismic wave propagation) is predicted using PGV, and pipe vulnerability caused by ground deformation (liquefaction or landslides) is predicted using PGD. In this study, the repair rate formula was utilized by multiplying the correction factor according to the pipe material and diameter considering the pipe damage owing to the ground shaking (Isoyama *et al.* 2000). The following equation expresses the repair rate using the correction factor:

$$Repair\ rate\ (RR_i) = C_1 C_2 \kappa (PGV_i)^{\tau} \tag{18}$$

where PGV_i represents the ground motion at the midpoint of the i-th pipe and κ and τ represent the scaling and exponential coefficients, respectively. The correction factors C_1 and C_2 are given by the pipe diameter and material type as shown in Table 1.

Previously proposed repair rates did not consider the deterioration of buried pipelines. As the seismic performance of a pipeline depends on the time elapsed since it has been buried, the repair rate of the pipeline must be modified according to the survival analysis of the pipeline. In this study, we introduce a modified repair rate using the survival function proposed by Park *et al.* (2010). The

Table 1 List of correction factors for different pipe materials and diameters

	Category	Factor		Category	Factor
Pipe material	Ductile iron	0.3	Pipe diameter	Φ75	1.6
	Cast iron	1.0		Φ100–150	1.0
	Polyvinyl	1.0		Φ200–450	0.8
	Steel	0.3		>Φ500~	0.5

modified repair rate (Fragiadakis and Christodoulou 2014; Yoon *et al*. 2018) can be expressed as follows

$$Modified\ repair\ rate\ (MRR_i) = \frac{1}{S(t)_{damaged}} C_1 C_2 \kappa (PGV_i)^{\tau} \quad (19)$$

where MRR_i is the modified repair rate of the i-th pipeline and $S(t)_{damaged}$ is the survival function of the buried pipe after buried time *t*. The failure probability of the buried pipeline based on the Poisson process can be expressed as follows:

$$P_{breakage,i} = 1 - e^{-MRR_i L_i} \quad (20)$$

where $P_{breakage,i}$ represents the breakage probability of the i-th pipe and L_i represents the length of the i-th pipeline. To consider leakage failure probability, Okumura and Shinozuka (1991) assumed that the probability of pipe leakage is five times that of the breakage failure. There are no reported data recorded separately for leakage and failure. Therefore, in this study, the pipeline leak probability proposed by Okumura and Shinozuka (1991) was considered as follows:

$$P_{leak,i} = 5 \times P_{breakage,i} \quad (21)$$

where $P_{leak,i}$ represents the leakage probability of the i-th pipe.

3.2.2 EPANET modelling of buried pipeline

To evaluate the required demand performance of the damaged water network, the entire network is simulated using the EPANET program by employing pressure-driven analysis (PDA). For numerical modelling of buried pipelines, damage states are classified into three types: leakage, breakage, and intact case. The broad approach proposed by Hwang *et al*. (1998) is adopted to evaluate the leakage and breakage conditions of damaged pipelines. In the EPANET analysis, an emitter is used to calculate the leakage and breakage discharge flows, and the emitter coefficient can be evaluated using the orifice flow rate equation. The following equation is the flow rate formula for obtaining the flow rate:

$$Q = Cp^{\gamma} \quad (22)$$

where p is the nodal pressure, C and γ are the emitter coefficient and exponent, respectively, and Puchovsky (1999) assumed γ to be 0.5 in the sprinkler model. When the Q of the above equation is substituted into the orifice flow rate equation (Gupta Ram 1989), the emitter coefficient can be calculated as follows:

$$C = C_0 A\sqrt{2g} \quad (23)$$

where C_0 is the orifice flow coefficient (empirically derived as 0.64), A is the cross-sectional area of the orifice, and g is the gravitational acceleration.

The outflow of the leakage or breakage pipeline is described using the orifice opening area and the orifice outflows are considered by updating the base nodal demand in the flow path. The outflow cross-sectional area of the orifice is assumed to be 3% when leakage occurs and 20% when breakage occurs (Farahmandfar and Piratla 2017). The cross-sectional area of the orifice owing to leakage and breakage can be expressed as follows:

$$A_{leak,i} = N_{leak,i} \times 0.03 \times A_i \quad (24)$$

$$A_{break,i} = N_{break,i} \times 0.2 \times A_i \quad (25)$$

where A_i represents the cross-sectional area of the i-th pipeline, and $N_{leak,i}$ and $N_{break,i}$ represent the numbers of leaks and breaks that can occur in the i-th pipeline, respectively.

Fig. 3 shows the procedure for calculating the orifice outflow rates for leakage and breakage of the pipeline. First, the orifice outflow rate is calculated using the average pressure at the end node of the pipe where the leakage and breakage occurred. Subsequently, the calculated orifice flow is newly assigned to the front node in the flow path and updated to the required nodal flow. In the case of leakage, only the orifice outflow is considered, whereas in the case of breakage, the orifice outflow is updated and the pipeline is closed. The revised nodal flow rate is as follows:

$$Q_{req,i} = Q_{base,i} + Q_{ori,i} \quad (26)$$

where $Q_{base,i}$ represents the base nodal demand of the i-th pipe, and $Q_{ori,i}$ represents the breakage and leakage discharge flow rate caused by the earthquake.

The EPANET program adopts demand-driven analysis (DDA), and the solver of the hydraulic analysis satisfies the nodal demands regardless of the nodal pressure. However, existing DDA methods have computational limitations to simulate unsteady state conditions, which can make the nodal pressure very low or even negative. Therefore, the PDA method is applied to evaluate the nodal pressure and nodal flow rate. The PDA method is a pressure-based analysis method that systematically reduces the nodal demands of the system through iterative calculation to treat the negative or low-pressure state. To estimate nodal serviceability, the head-flow relationship (HOR), which represents the relationship of the outflow rate according to each nodal pressure condition, should be determined. In this study, the HOR equation proposed by Wagner *et al*. (1988) nodal flow is obtained by multiplying the nodal serviceability ratio with the required nodal flow:

$$Nodal\ serviceability\ ratio\ (NSR_i) = \begin{cases} 0 & if\ P_{avl,i} < P_{min,i} \\ (\frac{P_{avl,i} - P_{min,i}}{P_{des,i} - P_{min,i}})^{1/n} & if\ P_{min,i} < P_{avl,i} < P_{des,i} \\ 1 & if\ P_{avl,i} > P_{des,i} \end{cases} \quad (27)$$

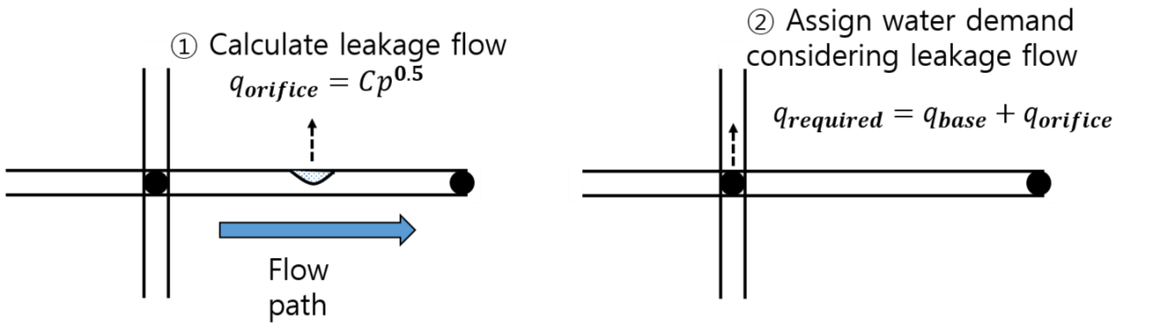

(a) leakage

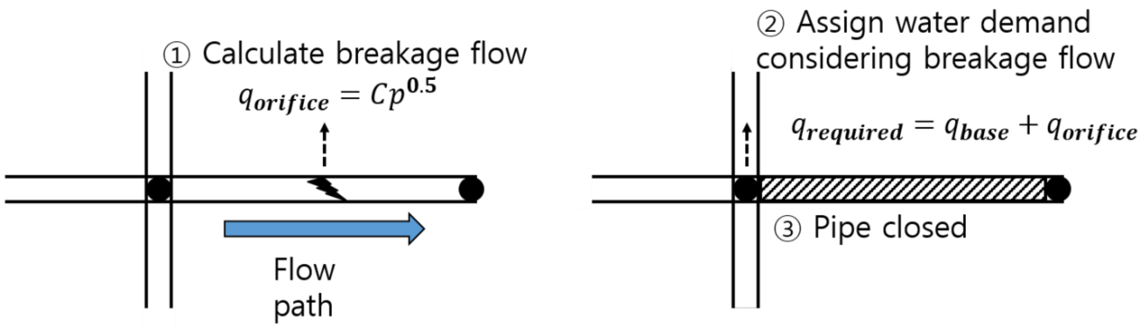

(b) breakage

Fig. 3 Numerical modelling of buried pipeline in EPANET analysis case of leakage and breakage

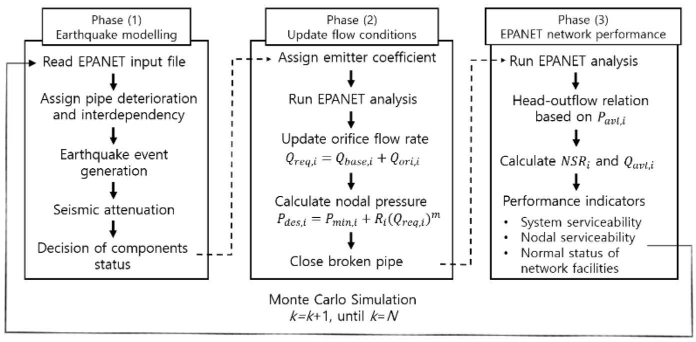

Fig. 4 Schematic diagram of flow-based seismic risk analysis of water network

$$Q_{avl,i} = Q_{req,i} \times NSR_i \tag{28}$$

where NSR_i represents the available flow rate ratio of the i-th node, $P_{min,i}$ is the minimum pressure required for the network (pressure head of 15 m in this study), and n is the serviceability coefficient between 1.5 and 2 (2 was utilized in this study). $P_{des,i}$ is the nodal pressure required to satisfy the required flow rate and can be calculated from the following equation (Gupta and Bhave 1996):

$$P_{des,i} = P_{min,i} + R_i(Q_{req,i})^m \tag{29}$$

where R_i is a resistance constant of the i-th node and m is the exponent coefficient. In this study, they were assumed to be 0.1 and 2, respectively (Gupta and Bhave 1996).

4. A comprehensive approach for flow-based probabilistic reliability model

In this section, a comprehensive approach for seismic risk analysis of a water transmission network is proposed. To evaluate seismic safety of a flow-based waterworks network, we implemented MATLAB computer code to enable EPANET hydraulic simulation with the PDA method. The flow-based probabilistic reliability model evaluates the network performance through the earthquake model phase and hydraulic analysis phase, and shows the performance indicators through the MCS process. Fig. 4 shows a three-phase flowchart of the numerical simulation used in this study. The basic process of the model is as follows:

Phase 1: The first step in the comprehensive approach is to build the EPANET input data and determine the deterioration and interdependency of facilities, including epicenter and the magnitude of the earthquake. If the location and magnitude of an earthquake are determined either probabilistically or deterministically, the ground motion prediction equation can be used to represent spatially correlated seismic intensity. From the calculated seismic intensity, the failure probability of the network facilities can be obtained. To determine the normal status of the network facilities, a random number between 0 and 1 is generated and compared with the failure probability. The facility is considered damaged if the generated random number is bigger than the failure probability; otherwise, the facilities maintain a normal status. Once all the network facilities have been determined, the results of the earthquake model and EPANET input file data are transferred to Phase 2.

Phase 2: The subsequent step is to calculate the orifice outflow from the leakage/breakage pipeline determined from Phase 1. First, EPANET analysis is performed to assign the emitter coefficient C according to the leakage or breakage state of the pipeline. When the orifice outflow $Q_{ori,i}$ is calculated, a new required flow rate $Q_{req,i}$ and the desired minimum pressure $P_{des,i}$ are updated to all nodes. The revised nodal flow and pressure are updated and the breakage pipeline is closed. Finally, the result of Phase 2 is transferred to Phase 3.

Phase 3: The final step is to evaluate the available nodal pressure and performance of the entire network using the input data from Phase 2. First, EPANET analysis is performed using the updated input file. By substituting the nodal available pressure $P_{avl,i}$ obtained from the hydraulic system into the HOR equation, the nodal serviceability ratio NSR_i and nodal available flow $Q_{avl,i}$ are obtained. Consequently, all the proposed performance indicators can be evaluated through $Q_{req,i}$, $P_{des,i}$, $P_{avl,i}$, and $Q_{avl,i}$. Phases 1 to 3 are considered as one MCS process, and MCS analysis is performed until the proposed performance indicators converge to account for the uncertainty of the reliability factor. The proposed performance indicators are calculated according to the location and magnitude of the earthquake, elapsed time of pipeline burial, and the interdependency between the pumping plant and the substation.

5. Seismic risk analysis of A-city water transmission network

5.1 Description of benchmark water network

For seismic risk analysis, it is important to obtain network operational data, GIS location information, and connectivity information of water supply facilities and substations. The network data for the waterworks were received from the A-city waterworks headquarter, and the location of the 154 kV substation was provided by the electric power company. Based on the provided data, a network map was reconstructed and used as the basic data of the input file in EPANET analysis. However, the GIS data of the underground facilities did not reveal specific information about the network owing to security issues.

The A-city water supply facilities provide water to 1,150,215 people (325562 m^3/day) in 1057 km^2 through two water treatment plants. Fig. 5 shows the supply process of water in A-city where purified water is supplied from the water source to the sink. In the water network, purified water is delivered to 23 water storage tanks through buried

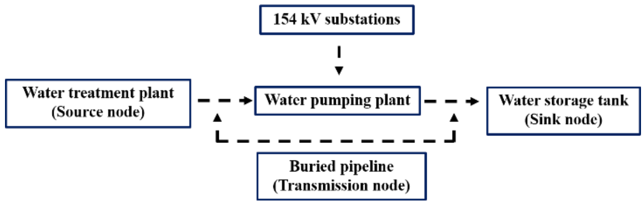

Fig. 5 Water supply process in A-city, South Korea

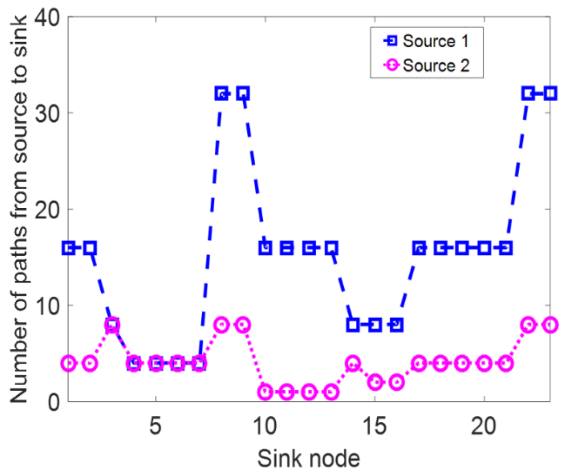

Fig. 6 Number of paths between water treatment plants and storage tanks

pipelines, and 17 pumping plants transport water to the highlands. The pumping plants are supplied with electric power from 10 substations. The network consists of 259 links and 264 nodes, and the total length of the pipeline is approximately 140.59 km (min: 41 m, max: 2922.3 m). With regard to pipeline materials, ductile cast iron pipes account for 71% of the total network and the remaining 29% are coated steel pipes. With regard to pipeline size, approximately 95% of the network has a pipe diameter of 500 mm or more, and approximately 5% of the network has a diameter of less than 500 mm (min: 300 mm, max: 1500 mm). Finally, the average elapsed time for the 259 pipelines is 15.2 years (min: 1 year, max: 32 years) as of 2016. Fig. 6 shows the number of paths connecting the source and each sink based on graph theory. In the case of a transmission network, most pipelines are connected in series, which indicates that the number of paths does not change significantly. In addition, the short number of paths from each source indicates close proximity, and Source 1 has more paths to access all sink nodes compared with Source 2.

In this study, based on the constructed network map, the epicenter was chosen to have a magnitude of 5.8, which occurred in B-city (nearest to A-city) in 2016. An analysis of historical seismic data showed that the selected earthquake was the largest earthquake that occurred close to A-city. An earthquake of magnitude 6.0–8.0 was generated using the epicenter of the selected input earthquake and the parametric study was performed by increasing the interdependency of the 154 kV substation and the pumping plant to 0, 0.5, and 1. Simultaneously, the elapsed time was increased from 0 to 30 years to evaluate the seismic

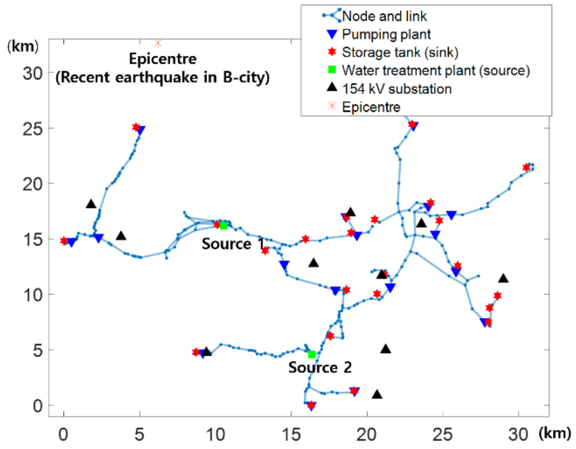

Fig. 7 Construction of water transmission network of A-city, South Korea

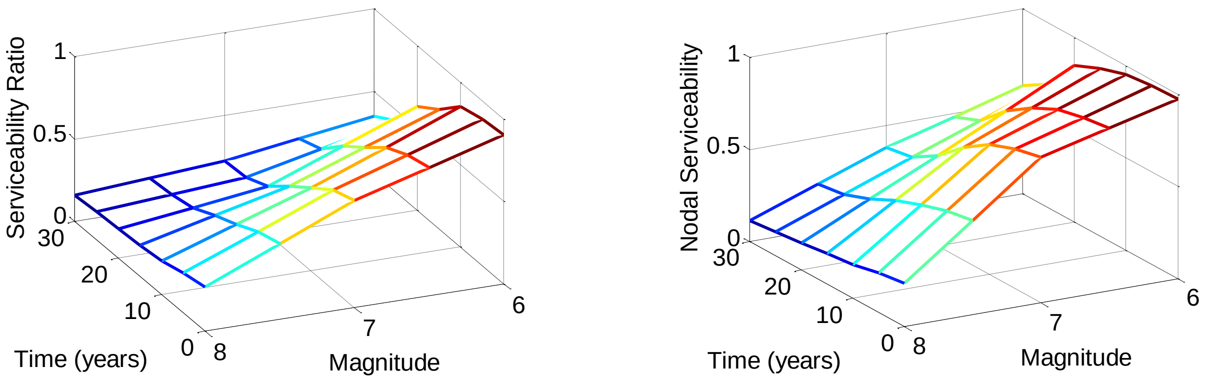

(a) Serviceability ratio (b) Nodal serviceability

Fig. 8 Seismic fragility surface of an independent water transmission network (a) Serviceability ratio (b) Nodal serviceability

performance of the water network owing to pipeline deterioration. The magnitude of the earthquake and the elapsed time were selected in consideration of the water pipe design standards in South Korea. Fig. 7 represents the entire water transmission networks and network facilities including 154 kV substations.

5.2 Evaluation of network performance

The first case study is the performance evaluation of a water supply system without considering the interdependency between the water pumping plants and the 154 kV substations. For numerical simulation, Phases 1–3 of the probabilistic reliability model proposed in Section 4 were used, and 10000 MCSs were performed to estimate the performance indicators for each event.

Fig. 8 shows the fragility surface of the system serviceability and nodal serviceability depending on the magnitude of the earthquake and elapsed time after burial. When an earthquake of magnitude 6.0 occurred, the system reliability of the entire network exceeded 0.95, and it was confirmed that stable water supply to the sink node was possible. However, as the magnitude of the earthquake increased to 7.0, the performance of the network decreased to 0.647, and when the magnitude of the earthquake was 8.0, the slope of the vulnerability surface tended to decrease more rapidly (drop to 0.257). This is because the greater the magnitude of the earthquake, the higher is the probability of failure of the water supply system and the more difficult it becomes to supply water in the closed state owing to pipeline failure. In addition, if the pipeline has been in service for more than 20 years, it can be observed that not only the magnitude of the earthquake but also the elapsed time after burial affects the network performance. This can be attributed to the fact that, even if the waterworks facilities are operated with stability, the buried pipelines are destroyed owing to deterioration during earthquakes of small magnitude (Park *et al.* 2010). As shown in Fig. 9, the NSL ratio decreases gradually as the magnitude of the earthquake increases, and the NSL performance declines sharply when the buried time is more than 20 years. These results show that, even though earthquakes of small magnitude satisfy the seismic design criteria, the performance of the pipeline itself owing to aging sufficiently affects the water network.

From the viewpoint of elapsed time of pipeline burial, the seismic performance of the network decreases with buried times. When the magnitude of the earthquake was 6.0, it was confirmed that the buried time significantly affected the network performance. However, as the

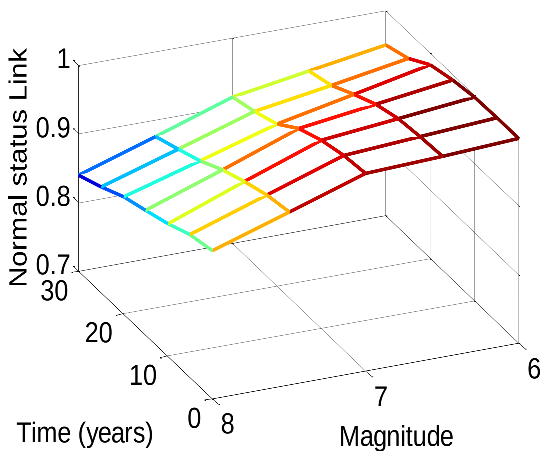

Fig. 9 Mean normal status rate of link depending on elapsed time and magnitude of earthquake

magnitude of the earthquake increased, the slope of the vulnerability surface tended to decrease with the elapsed time. This result shows that the breakage of the buried pipelines occurred sufficiently during earthquakes of magnitude 7.0–8.0 regardless of the pipeline deterioration. As observed from the NSL ratio, in an earthquake of magnitude 8.0, numerous pipelines are already in failure regardless of the elapsed time.

Fig. 10 shows the normal status ratio of the water treatment plant, pumping plant, and storage tank according to the magnitude of the earthquake. As the magnitude of the earthquake increases, the ratio of the facilities in the normal status decreases, especially for earthquakes of magnitude 7.0 and 8.0. However, the water storage tanks and pumping plants showed more than 80% stable state even if an earthquake of magnitude 8.0 occurred. The water treatment plant (source 1) located near the epicenter was measured to have a relatively low steady-state ratio, and the water treatment plant (source 2) located far away from the epicenter was more stable than source 1.

5.3 Evaluation of network performance considering electrical substation

In the second case study, seismic risk assessment was performed by considering the interdependency of substations supplying power to the pumping plants. As in Section 5.2, 10,000 MCS analyses were used to calculate the performance indicators and the system diagram of the substation supplying power to each pumping plant was used to account for the failure probability of 17 pumping plants.

Fig. 11 shows the fragility surface of the system serviceability and nodal serviceability of the network, depending on the magnitude of the earthquake, elapsed time, and interdependency ratio. Similar to the results described in Section 5.2, the network performance decreases as the magnitude of the earthquake increases and as the elapsed time increases. When the elapsed time was more than 20 years, the effects of the ground motion intensity and pipeline deterioration increased. In addition, it can be observed that the influence of the substation on the network performance becomes greater as the interdependency of the substation increases. In the case of the earthquake of magnitude 6.0, the performance variation owing to interdependency was not significant. However, as the magnitude of the earthquake increased to 7.0 and 8.0, the interdependency affected the network performance. The difference in network performance is related to the failure probability of the pumping plant according to the interdependency. Fig. 12 shows that the effect of interdependency is relatively small in low PGA range and the interdependency has a significant influence on the failure probability of pumping plants as the PGA increases.

The slope of the performance indicators tended to decrease sharply (M 6.0 to 7.0) when the interdependency was 0.5 (0.317) and 1 (0.375), compared with the case where the interdependency was 0 (0.241). However, when the magnitude of the earthquake increased from 7.0 to 8.0, the performance slope showed the sharpest change in the order of interdependency 0, 0.5, and 1. This is because, when the magnitude of the earthquake is 8.0, not only the effect of interdependency but also the failure of the pipeline owing to the ground motion occurs sufficiently. The interdependency when the earthquake of magnitude 8.0 (approximately 6–7%) occurred had a greater impact on the network performance than that of the earthquake of magnitude 6.0 (approximately 3–4%), but it was less than that of the earthquake of magnitude 7.0 (approximately 10–11%).

Fig. 12 shows the normal status ratio of the pumping plants. When the magnitude of the earthquake is 6.0, the normal status of the pumping plants has slight effect on the interdependency, but the effect of interdependency increases sharply as the magnitude of the earthquake increases. As observed from the failure possibility of the pumping plants, the interdependency has a significant effect as the PGA increases. As the normal status ratios of pipelines, storage tanks, and water treatment plants do not vary with interdependency, we used the results presented in Section 5.2.

6. Concluding remarks

In this paper, we propose a comprehensive approach to evaluate the flow-based seismic risk analysis of water transmission networks. The proposed method consists of three phases: earthquake generation model, update of orifice flow, and performance evaluation of water networks. To perform a hydraulic analysis, MATLAB-based computer code was developed and an actual water transmission network of South Korea was constructed. For numerical simulation, the epicenter was chosen based on historical data and the seismic performance was evaluated depending on the buried pipeline deterioration and the interdependency between water pumping plants and 154 kV substations.

The case studies focus on possible scenarios of the benchmark water network (location and magnitude of the earthquake) to enable an intuitive understanding of the methodology and results. The first case study deals with the evaluation of seismic performance without considering interdependency. The second case study is a performance

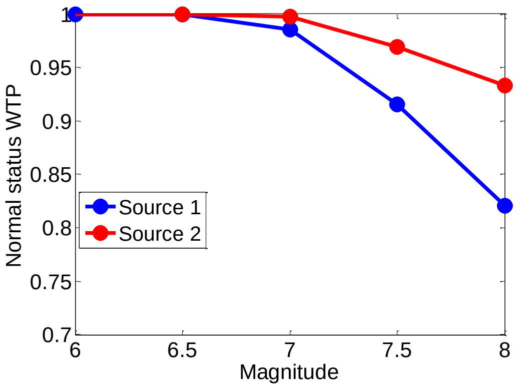

(a) Normal status of water treatment plant

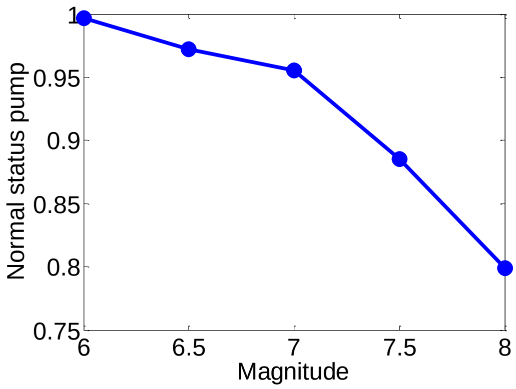

(b) Normal status of pumping plant

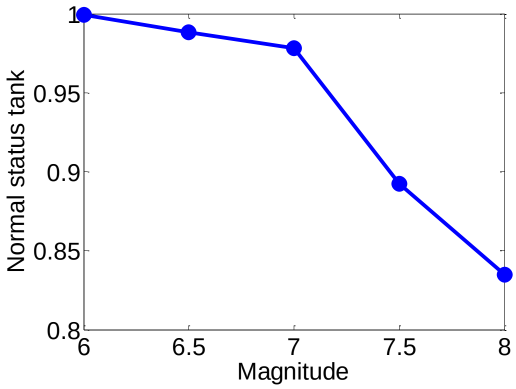

(c) Normal status of storage tank

Fig. 10 Mean normal status rate of other network facilities according to magnitude of earthquake

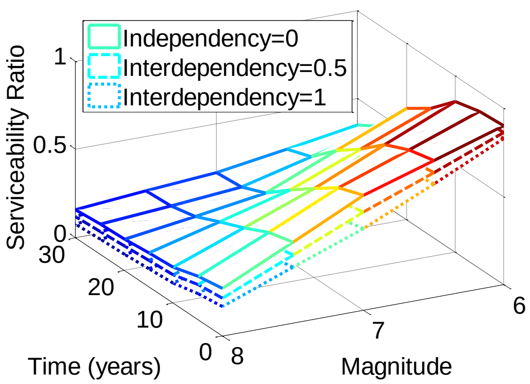

(a) Serviceability ratio

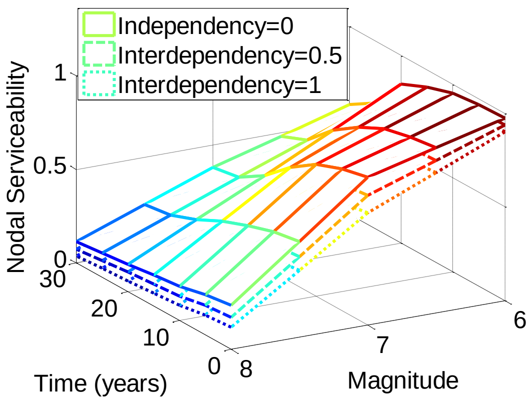

(b) Nodal serviceability

Fig. 11 Seismic fragility surface of water transmission network considering effects of power electric network

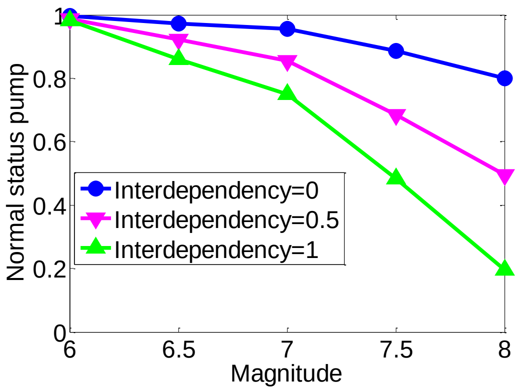

Fig. 12 Mean normal status rate of pumping plant according to interdependency

evaluation of waterworks facilities considering the interdependency of power generation facilities. In both cases, the network performance tended to decrease as the magnitude of the earthquake and elapsed time after burial increased. In addition, the interdependency, elapsed time after burial, and magnitude of the earthquakes have been observed to be closely related to the network performance Therefore, it is expected that consideration of the comprehensive impact of lifeline facilities will provide more insight for evaluating the performance of the network more accurately.

Until now, numerical simulations have been performed in terms of the service level of the nodal demands for the overall framework to be considered for evaluating the water transmission network. In the future, the results of this study could be applied to the prediction of post-hazard recovery time, estimation of direct and indirect damage, and optimal distribution of pipeline diameter.

Acknowledgments

The research described in this paper was financially supported by the Korea Institute of Energy Technology Evaluation and Planning (KETEP) and the Ministry of Trade, Industry & Energy (MOTIE) of the Republic of Korea (No. 20181510102410). This work was also financially supported by the National Research Foundation Korea (NRF) Grant funded by the Korean government (MSIP) (No. 2017R1A5A1014883).

References

Ahuja, R.K., Magnanti, T.L. and Orlin, J.B. (1993), *Network flows: theory, algorithms, and applications*, Prentice-Hall, Inc., New Jersey, U.S.A.

Bonneau, A.L. and O'Rourke, T.D. (2009), "Water supply performance during earthquakes and extreme events", MCEER Technical Report, MCEER-09-0003, National Science Foundation, Arlington, VA, U.S.A.

Cullinane, M.J., Lansey, K.E. and Mays, L.W. (1992), "Optimization-availability-based design of water-distribution networks", *J. Hydraulic Eng.*, **118**(3), 420-441. https://doi.org/10.1061/(asce)0733-9429(1992)118:3(420)

Dueñas-Osorio, L., Craig, J.I. and Goodno, B.J. (2007), "Seismic response of critical interdependent networks", *Earthq. Eng. Struct. Dynam.*, **36**(2), 285-306. https://doi.org/10.1002/eqe.626.

Esposito, S., Iervolino, I., d'Onofrio, A., Santo, A., Cavalieri, F. and Franchin, P. (2015), "Simulation-based seismic risk assessment of gas distribution networks", *Computer-Aided Civil Infrastructure Eng.*, **30**(7), 508-523. https://doi.org/10.1111/mice.12105

Farahmandfar, Z. and Piratla, K.R. (2017), "Comparative Evaluation of Topological and Flow-Based Seismic Resilience Metrics for Rehabilitation of Water Pipeline Systems", *J. Pipeline Syst. Eng. Practice*, **9**(1), 04017027. https://doi.org/10.1061/(asce)ps.1949-1204.0000293

FEMA (2003), Multi-hazard Loss Estimation Methodology Earthquake Model, HAZUS-MH MR3 Technical Manual, United States Department of Homeland Security, Federal Emergency Management Agency, Washington, D.C.

Fragiadakis, M. and Christodoulou, S.E. (2014), "Seismic reliability assessment of urban water networks", *Earthq. Eng. Struct. Dynam.*, **43**(3), 357-374. https://doi.org/10.1002/eqe.2348

Goda, K. and Atkinson, G.M. (2009), "Probabilistic characterization of spatially correlated response spectra for earthquakes in Japan", *Bullet. Seismologic. Soc. America*, **99**(5), 3003-3020. https://doi.org/10.1785/0120090007

Goda, K. and Hong, H.P. (2008), "Spatial correlation of peak ground motions and response spectra", *Bullet. Seismologic. Soc. America,* **98**(1), 354-365. https://doi.org/10.1785/0120070078

Gupta, R. and Bhave, P.R. (1996), "Comparison of methods for predicting deficient-network performance", *J. Water Resources Plan. Manage.*, **122**(3), 214-217. https://doi.org/10.1061/(asce)0733-9496(1996)122:3(214)

Gupta Ram, S. (1989), *Hydrology and Hydraulic System*, Prentice Hall, New Jersey, U.S.A.

Hwang, H.H., Lin, H. and Shinozuka, M. (1998), "Seismic performance assessment of water delivery systems", *J. Infrastructure Syst.*, **4**(3), 118-125. https://doi.org/10.1061/(asce)1076 0342(1998)4:3(118)

Isoyama, R., Ishida, E., Yune, K. and Shirozu, T. (2000), "Seismic damage estimation procedure for water supply pipelines", *Paper Proceedings of the 12th World Conference on Earthquake Engineering (WCEE)*, Auckland, New Zealand.

Joyner, W.B. and Boore, D.M. (1993), "Methods for regression analysis of strong-motion data", *Bullet. Seismologic. Soc. America*, **83**(2), 469-487.

Kang, W.H., Lee, Y.J. and Zhang, C. (2017), "Computer-aided analysis of flow in water pipe networks after a seismic event", *Math. Problems Eng.*, https://doi.org/10.1155/2017/2017046

Kashani, M.G., Hosseini, M. and Aziminejad, A. (2016), "Reliability evaluation of water distribution network considering mechanical characteristics using informational entropy", *Struct. Eng. Mech.*, **58**(1), 21-38. https://doi.org/10.12989/sem.2016.58.1.021

Kawashima, K., Aizawa, K. and Takahashi, K. (1984), "Attenuation of peak ground motion and absolute acceleration response spectra", *Proceedings of Eighth World Conference on Earthquake Engineering*, **362**, 169-176.

Kim, J.H., Lee, D.H. and Kang, J.H. (2019), "Multi-objective optimization of stormwater pipe networks and on-line stormwater treatment devices in an ultra-urban setting", *Membr. Water Treat.*, **10**(1), 75-82. https://doi.org/10.12989/mwt.2019.10.1.075

Lee, Y.J., Song, J., Gardoni, P. and Lim, H.W. (2011), "Post-hazard flow capacity of bridge transportation network considering structural deterioration of bridges", *Struct. Infrastruct. Eng.*, **7**(7-8), 509-521. https://doi.org/10.1080/15732479.2010.493338

Lim, H. W. and Song, J. (2012), Efficient risk assessment of lifeline networks under spatially correlated ground motions using selective recursive decomposition algorithm. *Earthquake Engineering & Structural Dynamics*, **41**(13), 1861-1882. https://doi.org/10.1002/eqe.2162

Nuti, C., Rasulo, A. and Vanzi, I. (2010), "Seismic safety of network structures and infrastructures", *Struct. Infrastruct. Eng.*, **6**(1-2), 95-110. https://doi.org/10.1080/15732470802663813

Okumura, T. and Shinozuka, M. (1991), "Serviceability analysis of Memphis water delivery system", *Proceedings of 3rd US Conference on Lifeline Earthquake Engineering*, Los Angeles, California.

Park, S., Choi, C.L., Kim, J.H. and Bae, C.H. (2010), "Evaluating the economic residual life of water pipes using the proportional hazards model", *Water Resources Management*, **24**(12), 3195-3217. https://doi.org/10.1007/s11269-010-9602-3

Puchovsky, M.T. (1999), *Automatic Sprinkler Systems Handbook*, National Fire Protection Association (NFPA), MA, U.S.A.

Rokneddin, K., Ghosh, J., Dueñas-Osorio, L. and Padgett, J.E. (2013), "Bridge retrofit prioritisation for ageing transportation networks subject to seismic hazards", *Struct. Infrastruct. Eng.*, **9**(10), 1050-1066. https://doi.org/10.1080/15732479.2011.654230

Romero, N., O'Rourke, T., Nozick, L. and Davis, C. (2010), "Seismic Hazards and Water Supply Performance", *J. Earthq. Eng.*, **14**(7), 1022-1043. https://doi.org/10.1080/13632460903527989

Sánchez-Silva, M., Daniels, M., Lleras, G. and Patiño, D. (2005), "A transport network reliability model for the efficient assignment of resources", *Transportation Res. Part B Methodological*, **39**(1), 47-63. https://doi.org/10.1016/j.trb.2004.03.002

Shi, P. and O'Rourke, T. D. (2006), "Seismic response modeling of water supply systems", MCEER Technical Report, MCEER-08-0016, Multidisciplinary Center for Earthquake Engineering Research, Buffalo, NY, U.S.A.

Sokolov, V., Wenzel, F., Jean, W.Y. and Wen, K.L. (2010), "Uncertainty and spatial correlation of earthquake ground motion in Taiwan", *Terr. Atmos*., https://doi.org/10.3319/tao.2010.05.03.01(t)

Song, J. and Ok, S.Y. (2010), "Multi-scale system reliability analysis of lifeline networks under earthquake hazards", *Earthq. Eng. Struct. Dynam.*, **39**(3), 259-279. https://doi.org/10.1002/eqe.938

Wagner, J.M., Shamir, U. and Marks, D.H. (1988), "Water Distribution Reliability: Simulation Methods", *J. Water Resources Plan. Manage.*, **114**(3), 276294. https://doi.org/10.1061/(asce)0733-9496(1988)114:3(276)

Wang, M. and Takada, T. (2005), "Macrospatial correlation model of seismic ground motions", *Earthq. Spectra*, **21**(4), 1137-1156. https://doi.org/10.1193/1.2083887

Wang, Y., Au, S.K. and Fu, Q. (2010), "Seismic risk assessment and mitigation of water supply systems", *Earthq. Spectra*, **26**(1), 257-274. https://doi.org/10.1193/1.3276900.

Wang, Y. and O'Rourke, T.D. (2006), "Seismic performance evaluation of water supply systems", MCEER Technical Report, MCEER-08-0015, Multidisciplinary Center for Earthquake Engineering Research, Buffalo, NY, U.S.A. https://doi.org/10.1193/1.3276900

Yoo, D. G., Jung, D., Kang, D., Kim, J. H. and Lansey, K. (2015), Seismic hazard assessment model for urban water supply networks. *J. Water Resources Plan. Manage.*, **142**(2), 04015055. https://doi.org/10.1061/9780784412947.092

Yoon, S., Lee, Y.J. and Jung, H.J. (2018), A comprehensive framework for seismic risk assessment of urban water transmission networks. *J. Disaster Risk Reduction*, **31**, 983-994. https://doi.org/10.1016/j.ijdrr.2018.09.002

CC